Effect of Para-Substituents and Solvent Polarity on the Formation of Triphenylboroxine·Amine Adducts

Jeremy Kua,* Matthew N. Fletcher, and Peter M. Iovine

Department of Chemistry, University of San Diego, 5998 Alcala Park, San Diego, California 92110

Received: April 3, 2006; In Final Form: May 15, 2006

Density functional theory (B3LYP//6-311+G*) calculations including Poisson−Boltzmann implicit solvent and NMR were used to study the formation of a series of para-substituted triphenylboroxine·amine adducts with respect to their phenylboronic acid monomers and free amine in solution. Our calculations suggest that the intermediate prior to forming trimer·amine is a dimer·amine adduct. Formation of dimer·amine can proceed via two pathways. Electron-donating substituents favor dimerization of two monomers before addition of the amine, and electron-withdrawing substituents favor formation of a monomer·amine adduct before addition of the second monomer. We also find that π-electron acceptors destabilize formation of the dimer and trimer with respect to its monomers. Electron-withdrawing substituents favor adduct formation. Adduct formation is enthalpically stabilized by increasing the polarity of the solvent but differential solubility of the monomer compared to trimer·amine also has an effect on the equilibrium constant.

Introduction

Boroxines, the dehydration product of organoboronic acids,[1] have found commercial use in such diverse areas as flame retardant materials,[2] dopants for lithium ion transference in polymer electrolytes,[3−5] acid alternatives in Suzuki−Miyaura coupling reactions,[6] and nonlinear optical materials.[7] Boroxines are known to form stable adducts with many nitrogen donor compounds including amines,[8−12] pyridines,[13] hydrazines,[14] azaindoles,[15] and even salen type ligands.[16] Low-temperature NMR studies on trimethylboroxine·ligand adducts indicate that the ligands are in fast exchange with activation barriers of 9−13 kcal/mol.[15,17]

There are few studies investigating the thermodynamics of boroxine formation. Tokunaga et al. measured the equilibrium constant between phenylboronic acid and triphenylboroxine for a series of *p*-phenyl substituents.[18] This equilibrium corresponds to step 1 in Figure 1. There have been two computational studies, one by us (summarized below), and the other by Beckmann et al. in which a ring strain argument is used to explain the stability of boroxine·ligand adducts.[19]

As arylboroxines find increased utility in material science applications, such as covalent organic frameworks[20] and nanoscale molecular scaffolds,[21] a firm understanding of fundamental arylboroxine solution chemistry, including the rich ligand chemistry, would facilitate progress. Although the ligand facilitated trimerization of arylboronic acids has been qualitatively reported, there have been no quantitative evaluations of this two-step process. As pointed out earlier, Tokunaga et al. investigated the thermodynamics of arylboroxine construction from monomeric arylboronic acids but did not address adduct formation. This computational and NMR-based study fills a gap in the literature of arylboroxines by systematically and quantitatively investigating the role of ligation in arylboroxine ring construction.

In our previous computational study,[22] we examined each individual step in the two-step reaction sequence: boroxine construction from monomeric boronic acids (step 1, Figure 1) and subsequent boroxine complexation by amines to form a 1:1 adduct (step 2, Figure 1). In that preliminary study we chose to use water as an implicit (but nonreactive) solvent because the implicit solvent parameters were well tested in the Jaguar[23] program. We found that the trimerization of phenylboronic acids to form arylboroxine rings (step 1) is enthalpically unfavorable. In contrast, the formation of stable 1:1 adducts (step 2) was highly favorable; in fact, sufficiently favorable to drive the two-step reaction forward toward formation of the products. Substitution of π-electron-withdrawing groups in the para-position of the phenyl ring further disfavored step 1, whereas the opposite was observed for π-electron-donors. On the other hand, substituents that were *overall* electron-withdrawing favored step 2, whereas electron donors disfavored it. We also found that formation of 1:2 adducts of arylboroxine·amine were less favorable enthalpically compared to 1:1 adducts.

We have extended the previous study to examine the thermodynamics of intermediate steps and identify potential stable intermediates using both computational methods and NMR. One possible intermediate in step 1 could be formation of a dimer from two boronic acid monomers. Furthermore, in the presence of ligand, it may be possible to form monomer·amine and dimer·amine, prior to the formation of trimer·amine. We seek to answer the following questions: (1) Can stable adducts be formed between the base and the monomer or dimer? (2) What is the lowest energy pathway to form the stable trimer·amine? (3) How do electron-acceptor and electron-donor substituents influence which reaction pathway will be most favorable enthalpically? (4) How does solvent polarity affect the thermodynamics of this system?

To complement our NMR studies, we have chosen to use three implicit solvents of varying polarity in our calculations: acetone, dichloromethane and chloroform. A selection of different *p*-phenyl substituents are used in the calculations (X = H, CH_3, OCH_3, F, Cl, $C(O)OCH_3$, $C(O)CH_3$, CHO, CN, CF_3). The six calculated compounds (monomer, dimer, trimer, and their 1:1 adducts) for each substituent are shown in Figure 2.

* Corresponding author. E-mail: jkua@sandiego.edu.

10.1021/jp062055e CCC: $33.50 © 2006 American Chemical Society
Published on Web 06/15/2006

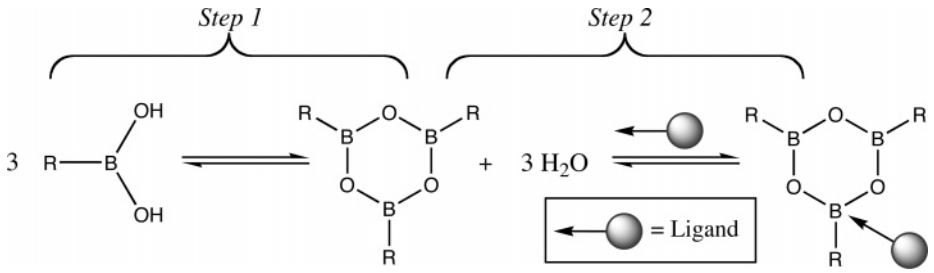

Figure 1. Two-step reaction sequence of boroxine construction followed by adduct formation.

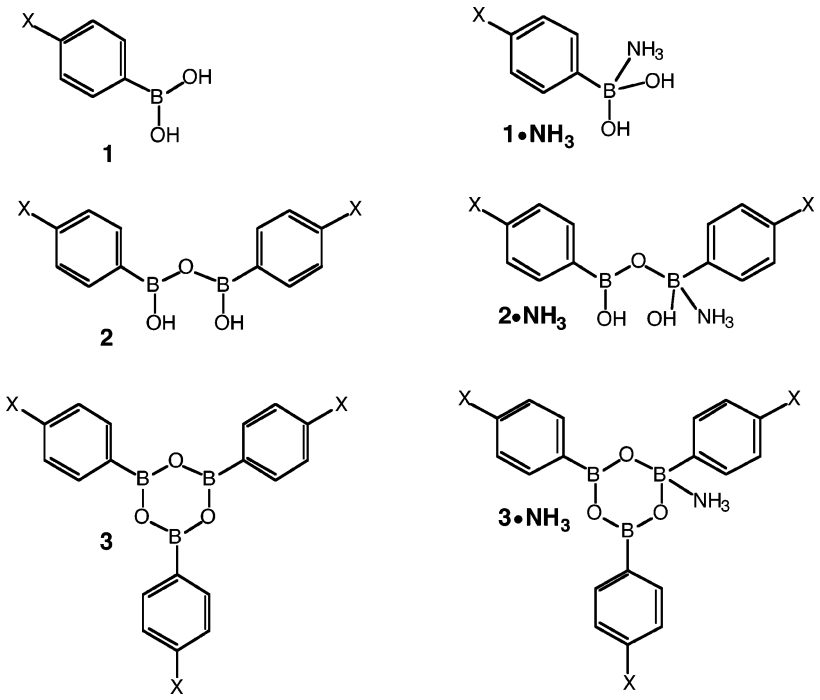

Figure 2. Compounds in this computational study.

In this study we have considered only 1:1 adducts because formation of 1:2 adducts were found to be much less favorable in our previous study.[22] For our calculations we have used the computationally less expensive NH_3 as the amine base. The NMR experiments use pyridine. A comparison between NH_3 and pyridine with respect to the thermodynamics for the formation of 1:1 adducts with arylboroxines can also be found in our previous study. In short, we found that trends were the same for both ligands, except that pyridine has a weaker binding energy to arylboroxine than NH_3.

Materials and Methods

Computational Methods. All calculations were carried out using Jaguar 5.5[23] at the B3LYP[24−27] flavor of density functional theory with a 6-311+G* basis set. We chose to run our calculations at a similar level of theory and basis set to complement our previous study.[22] The electronic energy of the optimized gas-phase structures is designated E_{elec}. The Poisson−Boltzmann (PB) continuum approximation[28,29] was used to describe the effect of solvent. In this approximation, a smooth solvent-accessible surface of the solute is calculated by rolling a sphere of radius R_{solv} over the van der Waals surface. The solvent is represented as a polarizable continuum surrounding the molecule with dielectric constant ϵ. The parameters used for the dielectric constant and probe radius are $\epsilon = 20.7$ and $R_{solv} = 2.43$ Å for acetone, $\epsilon = 10.0$ and $R_{solv} = 2.33$ Å for dichloromethane, $\epsilon = 4.8$ and $R_{solv} = 2.50$ Å for chloroform. Charges are allowed to develop on the surface according to the electrostatic potential of the solute and ϵ; then the polarized reaction field of the solvent acts back on the quantum mechanical description of the solute. The wave function of the complex is relaxed self-consistently with the reaction field to solve the PB equations. Although the forces on the quantum mechanical solute atoms due to the solvent can be calculated in the presence of the solvent, in this work, the solvation energy was calculated at the optimized gas-phase geometry. This is because there is little change between the gas-phase and implicit solvent optimized geometries. The difference in energy between the unsolvated and solvated structures is designated E_{solv}.

The analytical Hessian was calculated for each optimized geometry in the gas phase. The DFT gas-phase energy was then corrected for zero-point vibrations. The temperature-dependent enthalpy correction term is straightforward to calculate from statistical mechanics. Assuming that the translational and rotational corrections are a constant times kT, that low frequency vibrational modes will generally cancel out when calculating enthalpy differences, and that the vibrational frequencies do not change appreciably in solution, we can calculate H_{298K}. The sum of the zero point energy and enthalpy corrections to 298 K are collectively designated E_{corr}. The calculated values of E_{elec}, E_{solv} and E_{corr} are available in the Supporting Information. The corresponding free-energy corrections in solution are much less reliable.[30−32] Changes in free-energy terms for translation and rotation are poorly defined in solution, particularly as the size

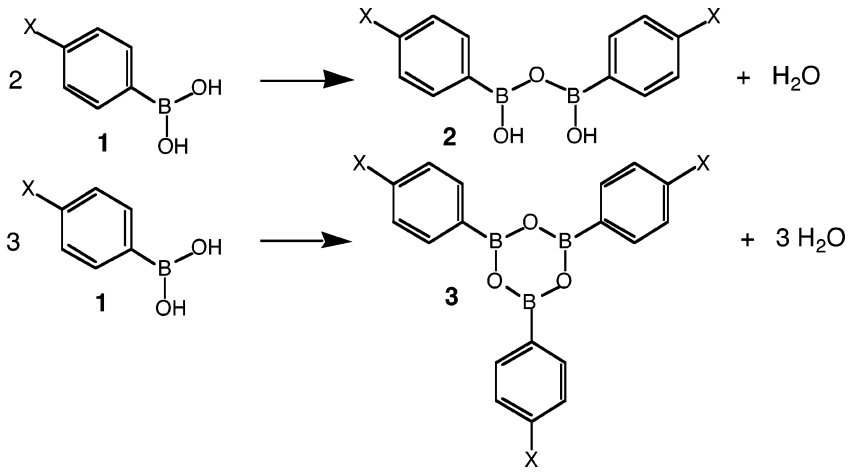

Figure 3. Dimerization and trimerization reactions of phenylboronic acid.

of the molecule increases. Additional corrections to the free energy for concentration differentials among species (to obtain the chemical potential) can be significant, especially if the solubility varies among the different species in solution. Furthermore, because the reactions being studied are in solution, the free energy being accounted for comes from two different sources: thermal corrections and implicit solvent. Neither of these parameters is easily separable, nor do they constitute all the required parts of the free energy under our approximations of the system.

Our reported reaction energies are as follows: (1) ΔE_{elec} is the difference in electronic energy between reactants and products in a given reaction. (2) ΔH_{gas} is calculated by adding zero point energy and thermal corrections to 298 K to the electronic energies. (3) ΔH_{soln} is calculated by adding the free energy due to solvation (for each solvent) to ΔH_{gas}. It is important to note that even though the solvation energy contribution is to some extent a free-energy correction, it certainly does not account for all of the free energy. Hence, we will retain the symbol ΔH and refer to this quantity as the solution phase enthalpy in our results and discussion.

Materials and Instrumentation. NMR data were acquired on a 400 MHz Varian Mercury system. All para-substituted phenylboronic acids were obtained from Frontier Scientific and used as received. The acetone-d_6 was purchased from Cambridge Isotope Labs in single-use ampules to minimize hydration. Pyridine was purchased from Acros Organics and was stored over 4 Å molecular sieves. Solvent chemical shifts for ^{1}H spectra are referenced to the deuterated solvent used in the experiment.

General Method for NMR Titration Measurements. Each para-substituted phenylboronic acid was added to a NMR tube as to give approximately 0.02 mmol. To the solid was added acetone-d_6 (0.5 mL), and a baseline spectrum was taken prior to the addition of the ligand. Pyridine (0.5 μL) was then added, and the tube shaken and rested for 10 min before a second ^{1}H NMR spectrum was acquired. The pyridine addition was repeated five times (total pyridine added was 3 μL), resulting in six ^{1}H NMR spectra for each para-substituted phenylboronic acid. The pyridine/boronic acid molar ratios were in the range of 0.33:1 to 2:1, respectively.

Assignment of the aromatic protons in 4-methoxyphenylboronic acid was made via a ROESY experiment.

The NMR spectra obtained after pyridine addition were integrated to determine concentrations of water, pyridine, monomeric boronic acid, arylboroxine, and pyridine·arylboroxine. The overall equilibrium constants for the two-step sequence outlined in Figure 1 were calculated using the following expression:

$$K = \frac{[H_2O]^3[\text{borox}\cdot\text{pyr}]}{[BA]^3[\text{pyr}]}$$

where [pyr] is the concentration of free pyridine, [borox·pyr] is the concentration of arylboroxine·pyridine, and [BA] is the concentration of the boronic acid monomer.

The downfield doublets associated with the boronic acid monomer and arylboroxine aromatic protons were well separated and therefore integrated separately. Because pyridine is in fast exchange on the NMR time scale, the aromatic protons corresponding to the arylboroxine species and the pyridine resonances are a weighted average of the bound and free species. However, under conditions where the ratio of pyridine/boronic acid was varied from 0.33:1 to 2:1, respectively, all arylboroxine was found to be bound. This observation was independently confirmed by monitoring the chemical shift of the arylboroxine/arylboroxine·pyridine's downfield aromatic doublet as a function of pyridine added. In the 0.33:1 to 2:1 pyridine/boronic acid range, the chemical shift of the downfield doublet did not shift, indicating that all arylboroxine present in solution was bound by pyridine. The integration of the arylboroxine·pyridine was then used to determine the concentration of bound versus unbound pyridine. In several cases, one of pyridine's three aromatic resonances overlapped with the downfield doublet of the boronic acid or arylboroxine·pryidine. In these instances, the two remaining pyridine resonances were used to deconvolute the overlap and isolate the portion of the integration originating from the boronic acid or arylboroxine·pyridine species.

Results and Discussion

Formation of Dimers and Trimers from Boronic Acid. The dimerization and trimerization reactions starting from boronic acid monomer **1** are shown in Figure 3. The dimer and arylboroxine trimer are labeled **2** and **3**, respectively. Calculated energies for the dimerization and trimerization reactions are compiled in Tables 1 and 2. The substituents have been sorted with respect to their Hammett parameters with the exception of CN and CF_3. We swapped the position of CN and CF_3 to group CN with the other π-acceptors. A graphical view of ΔH for the dimerization and trimerization reactions is represented by the left two columns (labeled 2x and 3x, respectively) in Figure 4.

TABLE 1: Energetics (kcal/mol) of Dimer Formation

X	ΔE_{elec}	ΔH_{gas}	ΔH_{soln}(acetone)	$\Delta H_{soln}(CH_2Cl_2)$	$\Delta H_{soln}(CHCl_3)$
OCH_3	2.54	2.20	2.93	2.57	2.29
CH_3	2.77	1.22	2.04	1.95	1.83
H	2.76	1.86	2.36	2.38	2.19
F	2.57	1.64	2.01	2.06	1.83
Cl	2.65	1.16	1.54	1.56	1.18
$C(O)OCH_3$	3.09	3.35	3.74	3.70	3.65
$C(O)CH_3$	3.08	3.34	3.73	3.73	3.42
CHO	3.07	3.32	3.64	3.61	3.36
CN	3.09	3.35	3.39	3.36	3.29
CF_3	3.18	3.44	3.70	3.80	3.70

TABLE 2: Energetics of Trimer Formation

X	ΔE_{elec}	ΔH_{gas}	ΔH_{soln}(acetone)	$\Delta H_{soln}(CH_2Cl_2)$	$\Delta H_{soln}(CHCl_3)$
OCH_3	12.45	9.69	2.82	3.28	4.08
CH_3	13.11	8.56	2.23	2.69	3.57
H	13.21	10.47	3.65	4.36	5.06
F	12.58	9.82	3.28	3.91	4.63
Cl	12.91	9.01	2.49	3.09	3.76
$C(O)OCH_3$	14.46	13.44	6.76	7.39	8.31
$C(O)CH_3$	14.67	13.67	6.66	7.39	8.00
CHO	14.76	13.75	6.78	7.40	8.15
CN	14.75	13.75	6.47	7.15	8.07
CF_3	14.58	11.80	4.76	5.53	6.35

All ΔH values are positive for both the dimerization and trimerization reactions. There is an average 88% increase (slightly less than double) in ΔH comparing the trimerization to the dimerization reaction for all substituents. This increase is most dramatic for π-accepting substituents in chloroform, the least polar of the solvents in our study. We find that:

(a) Substituents that are overall electron-donating, and $\pi-$donors in particular, result in ΔH values that are less positive than those for the unsubstituted case (X = H).

(b) The halogens (X = F, Cl), although overall electron-withdrawing, are good π-donors and have ΔH values less positive than X = H.

(c) Electron-withdrawing substituents, π-acceptors in particular, have ΔH values more positive than X = H.

(d) Comparing the different solvents we find that as the polarity of the solvent decreases, the change in solvation enthalpy becomes increasingly endothermic.

The dimerization reaction has equal numbers of reactants and products; thus we expect that the contribution of ΔS will be small (but not necessarily negligible given that the ΔH values are also relative small). The trimerization reaction releases three water molecules, so we expect ΔS to be positive and $-T\Delta S$ to be negative. Although we have not calculated free energies in solution, we expect ΔG values to still be positive, but smaller in magnitude than ΔH. The equilibrium constant measured via NMR spectroscopy (in $CDCl_3$) by Tokunaga et al.[18] suggest that the trimerization reaction is indeed thermodynamically unfavorable. Similar results were noted in our NMR experiments; however, our two-step solution measurements were performed in acetone instead of chloroform. Solvent appears to play an important role in the equilibrium, and therefore no direct comparison can be made between Tokunaga's NMR results and those presented here. This will be discussed in the next section.

In summary, we find that substitution of π-electron-withdrawing groups in the para-position of the phenyl ring further destabilize the dimer and trimer with respect to its monomers, whereas the opposite is observed from π-electron donors. We have previously compared and found good relative agreement between a subset of our calculated ΔE_{elec} values with $-RT \ln K_{eq}$ from experiment.[22]

Formation of 1:1 Adducts. Because trigonal planar boron can act as a Lewis acid, the addition of a Lewis base such as NH_3 may lead to the formation of 1:1 adducts. In the adduct, a new B−N bond is formed and boron adopts a tetrahedral environment. The base donates electron density to the tetrahedral boron, which in the Lewis structure carries a formal negative charge (nitrogen has the formal positive charge). Calculated energies for the addition of one equivalent of NH_3 to monomer, dimer and trimer to form 1:1 adducts are compiled in Tables 3−5. The adducts are labeled **1**·NH_3, **2**·NH_3 and **3**·NH_3 for the monomer, dimer and trimer, respectively. A graphical view of ΔH_{soln} for 1:1 adduct formation is represented by the middle three columns (labeled 1+NH_3, 2+NH_3, 3+NH_3, respectively) in Figure 4.

Three clear trends can be observed. The first trend is that the change in enthalpy is most favorable for the addition of NH_3 to the trimer and least favorable for adding NH_3 to the monomer. This comes as no surprise because the trimer has the greatest Lewis acidity and the monomer the least. ΔH is positive for the formation of **1**·NH_3, but for the more acidic dimer and trimer, ΔH is negative, indicating that forming the 1:1 adduct in solution is enthalpically favorable for dimers and trimers. Note that ΔS is negative for adduct formation; thus, $-T\Delta S$ will be positive and the entropic contribution disfavors adduct formation.

The second trend is that the exothermicity of adduct formation increases according to overall electron-withdrawing capability of the para-substituent. This holds true in all three solvents. This is not surprising because electron-donating groups are expected to destabilize the buildup of negative charge on the boron due to dative covalent bonding from the lone pair of ammonia. Electron-withdrawing groups, on the other hand, act to stabilize the adduct. The distinction between σ and π effects is not important once the adduct (with four-coordinate tetrahedral boron) is formed from a thermodynamic standpoint (although it may have a kinetic effect). Hence, we see that for adduct formation, the halogens act primarily in their electron-withdrawing capacity, stabilizing the build-up of negative charge on boron. Both F and Cl have ΔH values more exothermic than H. Because we have arranged the substituents according to their Hammett parameters (with the exception of CF_3 and CN), the middle three columns in Figure 4 highlight the trend toward increasing exothermicity with electron-withdrawing ability.

The third trend is that, as the polarity of the solvent decreases, ΔH_{soln} is less exothermic for forming **2**·NH_3 and **3**·NH_3 and more endothermic for forming **1**·NH_3. Because addition of NH_3 leads to a more polar compound (with formal B^- and N^+ charges), we would expect greater stabilization of the adduct with more polar solvents. This is indeed what we find in our calculations; however, this is not what is observed experimentally where more polar solvents (e.g., acetone) disfavor adduct formation relative to less polar solvents (e.g., chloroform). The 1:1 adduct with pyridine (experiment) is also less polar than with NH_3 (calculation).

Figure 5 shows the equilibrium distribution of 4-methoxyphenylboronic acid in acetone and chloroform. In both experiments one-third of an equivalent of pyridine (relative to the total molar quantity of boronic acid) was added to a solution of 4-methoxyphenylboronic acid. Because pyridine is known to be in fast exchange on the NMR time scale, the downfield doublet assigned to the arylboroxine (~7.8 ppm in acetone-d_6 and ~8.0 ppm in $CDCl_3$) actually represents a weighted average

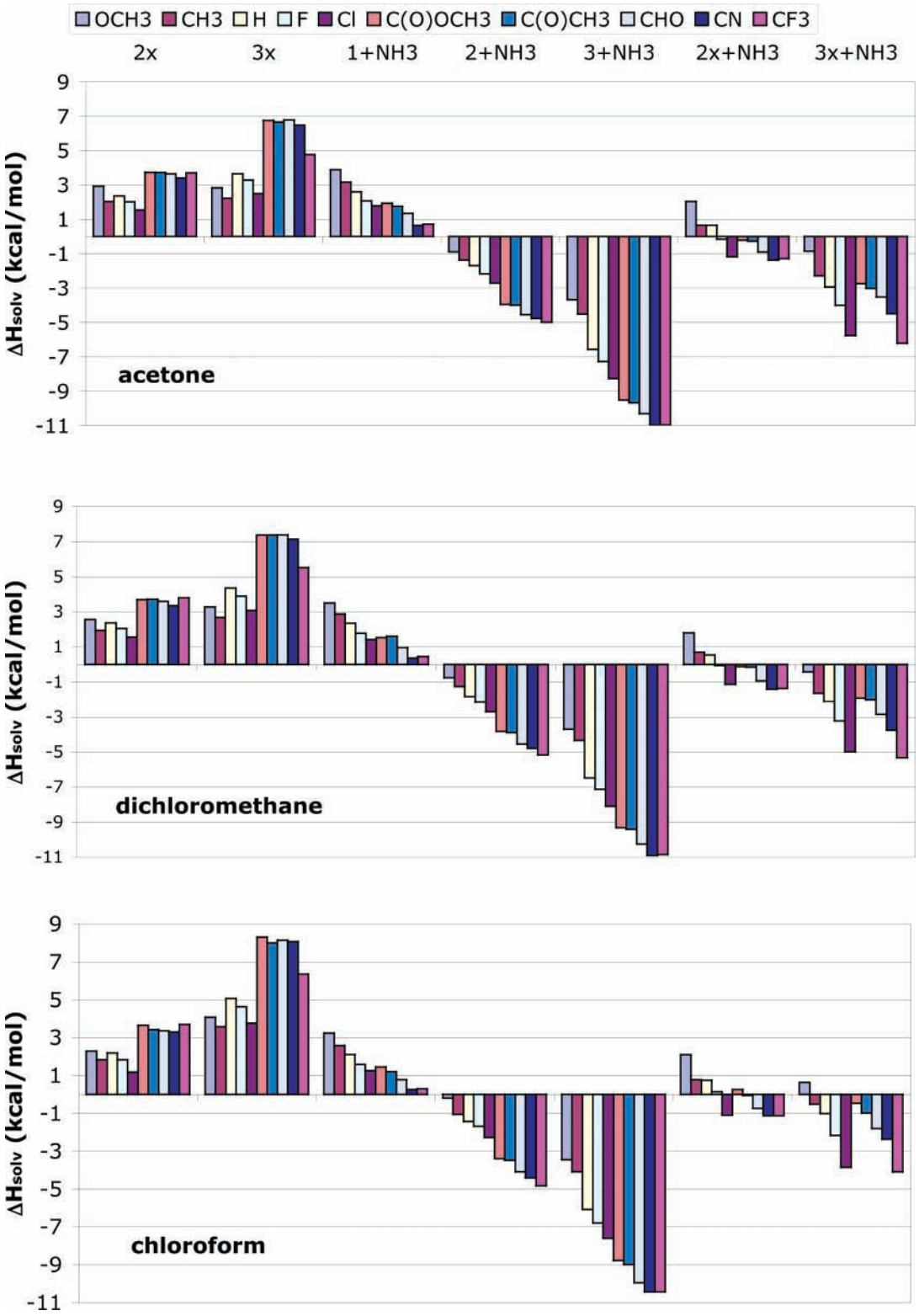

Figure 4. Calculated ΔH_{soln} (kcal/mol) for all reactions studied.

of ligated and unligated arylboroxine. Under the conditions of this experiment, arylboroxine was found to be fully bound by pyridine (see NMR Methods section). In acetone, a 4:1 ratio of boronic acid:arylboroxine·pyridine is observed. In chloroform, the major species is not the boronic acid but rather the arylboroxine·pyridine with an observed ratio of 1:2 boronic acid: arylboroxine·pyridine.

There are two factors that may play a role in causing the discrepancy between the computational results and experimental observations. The first issue relates to the inherent solubility of water in the two solvents and the ability of this dissolved water to participate in the ring-opening reaction. Practically speaking, acetone is much more difficult to obtain and maintain anhydrous and at low concentrations of substrate (~30 mM) trace water (as well as the extruded water from the condensation reaction) may be significant.

The second factor relates to the solubility of the starting boronic acid. At the concentrations used in this study, the

TABLE 3: Energetics (kcal/mol) of Formation of 1·NH_3

X	ΔE_{elec}	ΔH_{gas}	ΔH_{soln}(acetone)	ΔH_{soln}(CH_2Cl_2)	ΔH_{soln}($CHCl_3$)
OCH_3	0.58	2.37	3.88	3.51	3.24
CH_3	0.14	1.94	3.17	2.89	2.58
H	−0.32	1.51	2.60	2.36	2.11
F	−0.67	1.18	2.06	1.78	1.58
Cl	−1.00	0.87	1.78	1.43	1.26
$C(O)OCH_3$	−1.27	1.17	1.93	1.54	1.45
$C(O)CH_3$	−1.42	1.05	1.75	1.61	1.20
CHO	−1.94	0.55	1.35	0.97	0.77
CN	−2.32	0.20	0.64	0.37	0.25
CF_3	−1.96	−0.08	0.72	0.46	0.30

TABLE 4: Energetics (kcal/mol) of Formation of 2·NH_3

X	ΔE_{elec}	ΔH_{gas}	ΔH_{soln}(acetone)	ΔH_{soln}(CH_2Cl_2)	ΔH_{soln}($CHCl_3$)
OCH_3	−0.83	0.76	−0.89	−0.76	−0.20
CH_3	−1.98	0.27	−1.38	−1.25	−1.06
H	−2.59	−0.36	−1.70	−1.84	−1.44
F	−2.91	−0.64	−2.17	−2.13	−1.69
Cl	−3.41	−1.10	−2.72	−2.69	−2.28
$C(O)OCH_3$	−4.05	−1.77	−3.96	−3.82	−3.39
$C(O)CH_3$	−4.04	−1.75	−4.00	−3.88	−3.48
CHO	−4.83	−2.50	−4.55	−4.54	−4.10
CN	−5.40	−3.06	−4.77	−4.77	−4.42
CF_3	−5.18	−3.46	−4.99	−5.16	−4.83

TABLE 5: Energetics (kcal/mol) of Formation of 3·NH_3

X	ΔE_{elec}	ΔH_{gas}	ΔH_{soln}(acetone)	ΔH_{soln}(CH_2Cl_2)	ΔH_{soln}($CHCl_3$)
OCH_3	−4.46	−2.36	−3.68	−3.70	−3.45
CH_3	−5.60	−3.38	−4.52	−4.33	−4.09
H	−6.45	−4.25	−6.58	−6.47	−6.07
F	−6.93	−4.72	−7.29	−7.12	−6.80
Cl	−7.51	−5.22	−8.27	−8.08	−7.61
$C(O)OCH_3$	−8.45	−6.20	−9.51	−9.31	−8.78
$C(O)CH_3$	−8.63	−6.34	−9.68	−9.40	−8.99
CHO	−9.53	−7.20	−10.31	−10.24	−9.95
CN	−10.10	−7.73	−10.97	−10.90	−10.44
CF_3	−9.78	−7.99	−10.98	−10.85	−10.44

4-substituted-phenylboronic acid compounds are sparingly soluble in chloroform whereas in acetone, homogeneous solutions are formed. The addition of pyridine generally clarifies the chloroform solutions; i.e., arylboroxine·pyridine is soluble in chloroform. We think that the difference in solubility disfavors the reverse reaction (hydrolysis of arylboroxine back to monomer) because of an additional entropic cost due to phase separation of the sparingly soluble monomer from the solvent. Our calculations do not take this into account.

In all cases (except one: X = OCH_3 in chloroform), the exothermicity of ΔH for adduct formation is larger in magnitude than the endothermicity of ΔH for trimerization; i.e., the presence of NH_3 favors stabilization of the arylboroxine ring via adduct formation. In the absence of NH_3, formation of the arylboroxine ring is disfavored by an increasingly endothermic ΔH. This is also the trend observed in the experimental data. Only after adding a suitable ligand, in our case pyridine, is the equilibrium shifted substantially toward the arylboroxine products. The net result from adding these two ΔH values is represented graphically by the rightmost column in Figure 4 (labeled 3x+NH_3). This net ΔH value is obtained by adding ΔH values from the second (labeled 3x) and fifth (labeled 3+NH_3) columns. The overall net reaction is shown in Figure 6 and the net ΔH values are compiled in Table 6.

The most exothermic net ΔH values come from the CF_3 and Cl substituents. CF_3 is very strongly electron withdrawing, thus stabilizing the build-up of negative charge on boron in the adduct. Although the π-electron-withdrawing substituents ($C(O)OCH_3$, $C(O)CH_3$, CHO, CN) also strongly stabilize adduct formation, they decrease the stability of the trimer relative to its monomers; they have the most endothermic ΔH values for forming **3** (Table 2, second column in Figure 4). The halogens, on the other hand, as π-donors, are less endothermic toward trimer formation, and their overall electron-withdrawing capability (though weaker than that of the π-acceptors in this study) leads to significant stabilization of **3**·NH_3.

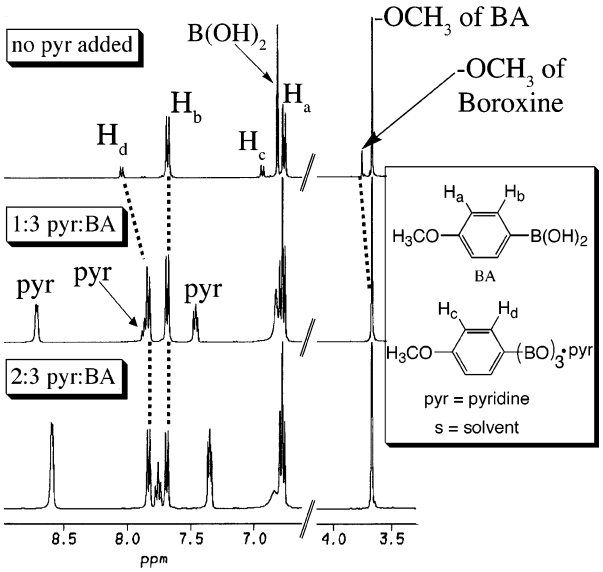

Figure 5. ^{1}H NMR spectra of 4-methoxyphenylboronic acid in the presence of pyridine comparing the equilibrium distribution of species as a function of solvent.

The overall two-step equilibrium (Figure 1) associated with arylboroxine formation and ligation was also examined by ^{1}H NMR spectroscopy. To our knowledge this is the first experimental study to quantify the thermodynamics of the two-step equilibrium process.

Figure 7 shows a representative titration experiment for 4-methoxyphenylboronic acid in acetone. The top spectrum (Figure 7, top panel), in the absence of the pyridine ligand, shows a mixture of 4-methoxyphenylboronic acid (labeled with circles) and 4-methoxyphenylboroxine (labeled with triangles). In the absence of pyridine the monomeric boronic acid dominates. Of particular interest are the downfield sets of aromatic protons (8.2−7.5 ppm) as the chemical shifts associated with these protons are diagnostic of the structure (i.e., arylboroxine·pyridine, arylboroxine, boronic acid). The boronic acid −OH resonance appears as a sharp singlet at approximately 6.8 ppm in the top spectrum.

The middle spectrum results from the addition of 1 equiv of pyridine relative to 3 molar equiv of monomeric boronic acid. The presence of the ligand drives the formation of the arylboroxine ring and the downfield doublet associated with the arylboroxine moves upfield. Using this experimental approach, equilibrium values and the corresponding ΔG values were determined for a series of para-substituted compounds. The results are presented in Table 7.

The free energy trends in the NMR data are in general agreement with the trends observed in the computational portion of the study. The most electron-donating substituent, OCH_3, has the least negative free energy change. H and CH_3 are very close. The electron-withdrawing substituents have a more negative free energy change than X = H. Note that the computational results are in terms of enthalpy changes rather than free energy changes; entropic and solubility effects were not included. Therefore, it is not unexpected that there are some differences in the trend. In the computational study, X = CH_3 (being mildly electron

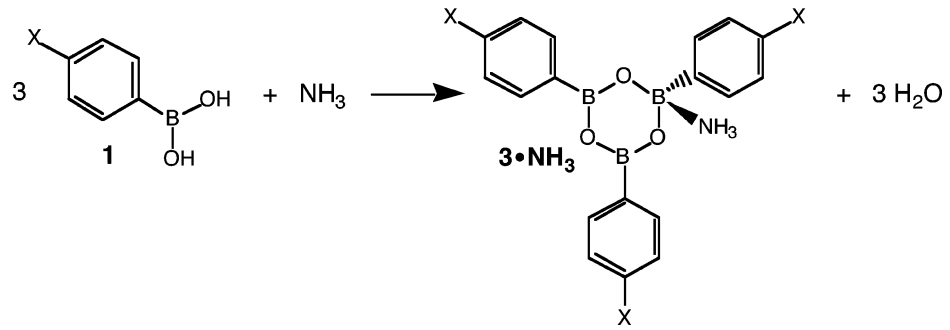

Figure 6. Net reaction for forming **3**·NH_3 when monomers and NH_3 are present.

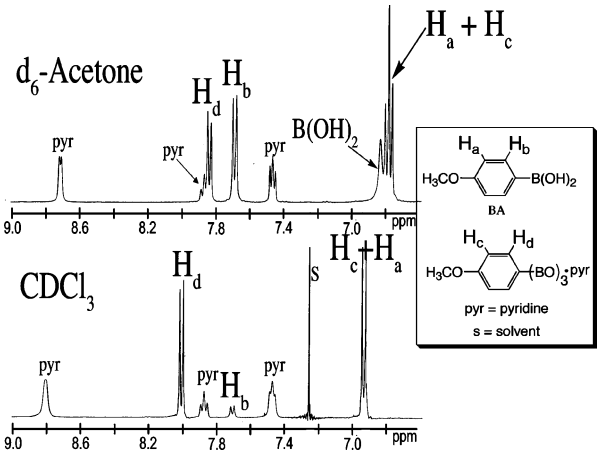

Figure 7. ^1H NMR stack plot in acetone-d_6 showing the equilibrium distribution of species for 4-methoxyphenylboronic acid as a function of pyridine added.

TABLE 6: Net ΔH (kcal/mol) for Forming 3·NH_3 When Monomers and NH_3 Are Present

X	ΔH_{soln}(acetone)	$\Delta H_{soln}(CH_2Cl_2)$	$\Delta H_{soln}(CHCl_3)$
OMe	−0.86	−0.42	0.63
CH_3	−2.29	−1.64	−0.52
H	−2.93	−2.11	−1.01
F	−4.01	−3.21	−2.17
Cl	−5.78	−4.99	−3.85
$C(O)OCH_3$	−2.75	−1.92	−0.47
$C(O)CH_3$	−3.02	−2.01	−0.99
CHO	−3.53	−2.84	−1.80
CN	−4.50	−3.75	−2.37
CF_3	−6.22	−5.32	−4.09

TABLE 7: NMR-Based Thermodynamic Data Acquired in acetone-d_6 for the Two-Step Equilibrium Process Shown in Figure 1

X	net equilibrium constant (step 1 and 2 from Figure 1)	ΔG (kcal/mol)
OCH_3	1.4	−0.2
H	2.8	−0.6
CH_3	3.3	−0.7
$C(O)CH_3$	10.0	−1.3
CF_3	11.0	−1.4
CN	16.0	−1.7

donating) was less exothermic than X = H, although the differences in experimental ΔG and computational ΔH comparing both substituents were both very small. The other difference is that X = CF_3 was found to be more exothermic than X = CN computationally.

In summary, overall electron-withdrawing ability is important in stabilizing formation of **3**·NH_3. Formation of this adduct was found to be overall exothermic in almost all cases. The value of ΔH represents a balance between the relative energy of **3** with respect to its monomers (favorable for π-donors, unfavorable for π-acceptors) and stabilization of **3**·NH_3 (favorable for overall electron-withdrawing substituents).

Relative Importance of 2·NH_3 as an Intermediate. How does the reaction proceed from monomers and free NH_3 in solution to formation of **3**·NH_3, the thermodynamic sink in this system? Our results suggest that forming the trimer in the absence of base is highly unfavorable, as **3** is the highest energy stable intermediate among all possible species. Instead, our calculations point to **2**·NH_3 as the most likely intermediate prior to formation of **3**·NH_3. The formation of **2**·NH_3 from monomers and free NH_3 in solution is shown in Figure 8. The net ΔH values for this reaction are represented by the second rightmost column in Figure 4 (labeled 2x+NH_3) and are the sum of ΔH values from Tables 1 and 4 (or the first and fourth columns of Figure 4 labeled 2x and 2+NH_3, respectively). These net values are shown in Table 8.

The net ΔH values are slightly endothermic for electron-donating substituents and X = H. For electron-withdrawing substituents, these values are marginally exothermic with two exceptions (X = F, $C(O)OCH_3$ in chloroform). Note that ΔS is negative in this reaction; thus, $-T\Delta S$ will be positive and the entropic contribution is likely to lead to positive ΔG values for all substituents except those with the most exothermic ΔH values (X = CF_3, CN, Cl). Thus the dimer adduct is unlikely to be observed unless the substituent is strongly electron withdrawing (and preferably through the σ-framework). Preliminary ^1H and ^{19}F NMR data obtained for *p*-(trifluoromethyl)phenylboronic acid may support this hypothesis (see Supporting Information where an additional set of signals is tentatively assigned to the dimer adduct).

There are two possible ways to get to **2**·NH_3 from monomers and free NH_3: (1) dimerization of the monomers first, followed by addition of NH_3 to the dimer; (2) addition of NH_3 to the monomer first, followed by addition of the second monomer. These two routes are shown in Figure 9. To compare the favorability of these two routes, we can compare the relative ΔH values for the first step in each route, i.e., comparing the results in Table 1 to those in Table 3, or the first column in Figure 4 (labeled 2x) with the third column (labeled 1+NH_3). Both of these first steps are endothermic.

We find that ΔH is less endothermic for dimerization as the first step for electron-donating substituents and X = H. On the other hand, the electron-withdrawing substituents have a less endothermic ΔH compared to X = H for adding NH_3 to the monomer as the first step. This suggests that the choice of substituent can play a role in which pathway is taken: electron donors favor the top pathway in Figure 9 and electron acceptors prefer the bottom pathway.

The argument above only considered the enthalpic contribution of the first step of the reaction. The entropic contribution

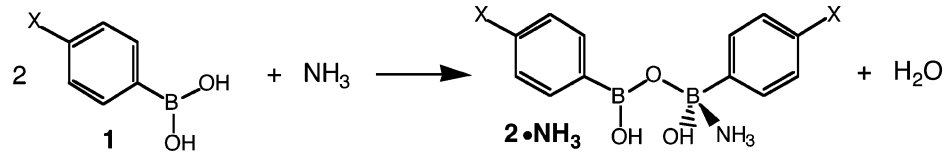

Figure 8. Net reaction for forming **2**·NH_3 from monomers and free NH_3.

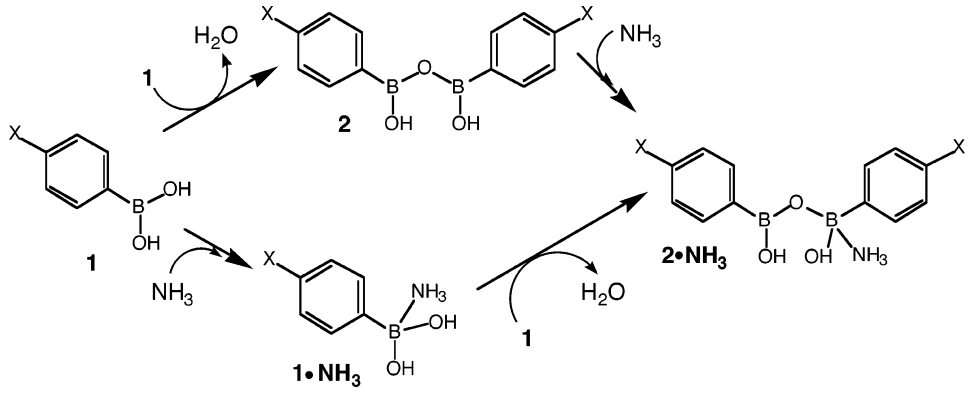

Figure 9. Routes to formation of **2**·NH_3 from monomers and free NH_3.

TABLE 8: Net ΔH (kcal/mol) for Forming 2·NH_3 When Monomers and NH_3 Are Present

X	ΔH_{soln}(acetone)	$\Delta H_{soln}(CH_2Cl_2)$	$\Delta H_{soln}(CHCl_3)$
OCH_3	2.04	1.81	2.09
CH_3	0.66	0.70	0.77
H	0.66	0.54	0.75
F	−0.16	−0.07	0.14
Cl	−1.18	−1.13	−1.10
$C(O)OCH_3$	−0.22	−0.12	0.26
$C(O)CH_3$	−0.27	−0.15	−0.06
CHO	−0.91	−0.93	−0.74
CN	−1.38	−1.41	−1.13
CF_3	−1.29	−1.36	−1.13

is expected to further destabilize formation of the monomer 1:1 adduct (bottom pathway) and have less of an effect on dimerization; the latter having equal numbers of moles of reactants and products. The activation barrier in each case may also have a significant effect on the pathway taken. We are currently working on optimizing all the low-lying transition states and calculating the barriers in this system. Preliminary estimates suggest that the barriers for each step in both pathways are low (in the range 6−14 kcal/mol), with addition of base to form an adduct having lower barriers than coupling of monomers to form dimer. NMR data are supportive of low barriers as (1) the addition of base proceeds completely to the thermodynamic sink, therefore suggesting equlilibration at room temperature, and (2) pyridine is in fast exchange on the NMR time scale. These points mesh well with the low dissociation/association activation barrier (approximately 10 kcal/mol) reported for the phenylboroxine•pyridine system.[15]

Conclusions

From our DFT calculations we find that in the absence of base, formation of dimers and trimers is thermodynamically unfavorable. Para substituents that are π-acceptors have the greatest destabilizing effect for forming dimers and trimers. For formation of adducts **1**·NH_3, **2**·NH_3 and **3**·NH_3 from **1**, **2** and **3**, respectively, with free NH_3, we find that the electron-withdrawing ability of a substituent correlates well with its ability to stabilize the adduct. Although the formation of **1**·NH_3 is calculated to be endothermic, formation of **2**·NH_3 and **3**·NH_3 are calculated to be exothermic. Our NMR data provided independent confirmation that electron-withdrawing substituents do drive the two-step equilibrium toward adduct formation, in agreement with our computational results.

We also find, from our calculations of ΔH, that the most important intermediate prior to forming **3**·NH_3 is **2**·NH_3. Formation of **2**·NH_3 can proceed via two pathways. Electron-donating substituents favor dimerization of two monomers before addition of NH_3, and electron-withdrawing substituents favor formation of a **1**·NH_3 before addition of the second monomer. Entropic effects may possibly change these results.

As the solvent increases in polarity from chloroform to dichloromethane to acetone, formation of trimer in the absence of NH_3 decreases in endothermicity, whereas formation of the more polar adducts in the presence of NH_3 is further stabilized. As entropic effects and phase separation are not included in our calculations, it is not surprising that our calculated trend of ΔH is different from that observed by NMR.

We are in the process of calculating activation energy barriers between these intermediates, and determining the geometric structure of the relevant transition states.

Acknowledgment. This research was supported by a Camille and Henry Dreyfus Foundation Start-up Award (J.K.), University of San Diego startup funds (J.K.), awards from Research Corporation (P.M.I., J.K.) and the American Chemical Society Petroleum Research Fund (40382-GB4) (P.M.I.). NSF MRI CHE-0417731 (P.M.I) is also acknowledged.

Supporting Information Available: Calculated values of E_{elec}, E_{solv} and E_{corr}, and preliminary ^1H and ^{19}F NMR data supporting the existence of a pyridine·boronic acid dimer adduct. This material is available free of charge via the Internet at http://pubs.acs.org.

References and Notes

(1) Hall, D. G. *Boronic Acids*; Wiley-VCH: New York, 2005.
(2) Morgan, A. B.; Jurs, J. L.; Tour, J. M. *Polym. Prepr. (Am. Chem. Soc., Div. Polym. Chem.)* **1999**, *40*, 553.
(3) Mehta, M. A.; Fujinami, T. *Chem. Lett.* **1997**, 915.
(4) Yang, Y.; Inoue, T.; Fujinami, T.; Mehta, M. A. *J. Appl. Polym. Sci.* **2002**, *84*, 17−21.
(5) Forsyth, M.; Sun, J.; Zhou, F.; MacFarlane, D. R. *Electrochim. Acta* **2003**, *48*, 2129.
(6) Miyaura, N.; Suzuki, A. *Chem. Rev.* **1995**, *95*, 2457.

(7) Alcaraz, G.; Euzenat, L.; Mongin, O.; Katan, C.; Ledoux, I.; Zyss, J.; Blanchard-Desce, M.; Vaultier, M. *Chem. Commun.* **2003**, *22*, 2766.
(8) Fielder, W. L.; Chamberlain, M. M.; Brown, C. A. *J. Org. Chem.* **1961**, *26*, 2154.
(9) Branch, G. E. K.; Yabroff, D. L. *J. Am. Chem. Soc.* **1932**, *54*, 2569.
(10) Mariategui, J. F.; Niedenzu, K. *J. Organomet. Chem.* **1989**, *369*, 137.
(11) Beckett, M. A.; Strickland, G. C.; Varma, K. S.; Hibbs, D. E.; Hursthouse, M. B.; Malik, K. M. A. *J. Organomet. Chem.* **1997**, *535*, 33.
(12) Ritchey, J. M. Synthesis and Properties of Addition Complexes of Boroxines and Other Selected Boron-Containing Systems. Ph.D. Thesis. University of Colorado, 1968.
(13) Snyder, H. R.; Konecky, M. S.; Lennarz, W. J. *J. Am. Chem. Soc.* **1958**, *80*, 3611.
(14) Das, M. K.; Mariategui, J. F.; Niedenzu, K. *Inorg. Chem.* **1987**, *26*, 3114.
(15) Wu, Q. G.; Wu, G.; Brancaleon, L.; Wang, S. *Organometallics* **1999**, *18*, 2553.
(16) Vargas, G.; Hernandez, I.; Hopfl, H.; Ochoa, M.-E.; Castillo, D.; Farfan, N.; Santillan, R.; Gomez, E. *Inorg. Chem.* **2004**, *43*, 8490.
(17) Beckett, M. A.; Brassington, D. S.; Owen, P.; Hursthouse, M. B.; Light, M. E.; Malik, K. M. A.; Varma, K. S. *J. Organomet. Chem.* **1999**, *585*, 7.
(18) Tokunaga, Y.; Ueno, H.; Shimomura, Y.; Seo, T. *Heterocycles* **2002**, *57*, 787.
(19) Beckmann, J.; Dakternieks, D.; Duthie, A.; Lim, A. E. K.; Tiekink, E. R. T. *J. Organomet. Chem.* **2001**, *633*, 149.
(20) Cote, A. P.; Benin, A. I.; Ockwig, N.; O'Keefe, M.; Matzger, A. J.; Yaghi, O. M. *Science* **2005**, *310*, 1166.
(21) Perrtu, E. K.; Arnold, M.; Iovine, P. M. *Tetrahedron Lett.* **2005**, *46*, 8753.
(22) Kua, J.; Iovine, P. M. *J. Phys. Chem. A* **2005**, *109*, 8938.
(23) *Jaguar v5.5*; Schrodinger, LLC: Portland, OR, 2003.
(24) Becke, A. D. *J. Chem. Phys.* **1993**, *98*, 5648.
(25) Becke, A. D. *Phys. Rev. A* **1988**, *38*, 3098.
(26) Vosko, S. H.; Wilk, L.; Nusair, M. *Can. J. Phys.* **1980**, *58*, 1200.
(27) Lee, C.; Yang, W.; Parr, R. G. *Phys. Rev. B* **1988**, *37*, 785.
(28) Tannor, D. J.; Marten, B.; Murphy. R.; Friesner, R. A.; Sitkoff, D.; Nicholls, A.; Ringnalda, M.; Goddard, W. A., III; Honig, B. *J. Am. Chem. Soc.* **1994**, *116*, 11875.
(29) Marten, B.; Kim, K.; Cortis, C.; Friesner, R. A.; Murphy, R. B.; Ringnalda, M. N.; Sitkoff, D.; Honig, B. *J. Phys. Chem.* **1996**, *100*, 11775.
(30) Wiberg, K. B.; Bailey, W. F. *J. Am. Chem. Soc.* **2001**, *123*, 8231.
(31) Nielsen, R. J.; Keith, J. M.; Stoltz, B. M.; Goddard, W. A., III. *J. Am. Chem. Soc.* **2004**, *126*, 7967.
(32) Florian, J.; Warshel, A. *J. Phys. Chem. B* **1998**, *102*, 719.